



ARTICLE

Numerical-Experimental Analysis of the Coal Fracture Formation Mechanism Induced by Liquid CO₂ Explosion

Yun Lei^{1,2,*}

¹Shenyang Research Institute, China Coal Technology & Engineering Group Corp., Fushun, 113122, China

²State Key Laboratory of Coal Mine Safety Technology, Fushun, 113122, China

*Corresponding Author: Yun Lei. Email: leiyun_123@163.com

Received: 27 February 2023 Accepted: 05 May 2023 Published: 27 October 2023

ABSTRACT

The highly inefficient simultaneous extraction of coal and gas from low-permeability and high-gas coal seams in deep mines is a major problem often restricting the sustainable development of coal industry. A possible way to solve this problem under deep and complex geological conditions is represented by the technology based on the phase-change induced explosion of liquid carbon dioxide. In this work, the mechanism of formation of the coal mass fracture circle resulting from the gas cracking process is theoretically analyzed. Numerical simulations show that a blasting crushing zone with a radius of 1.0 m is formed around the blasting hole. The radius of the secondary expansion zone caused by the exploding gas is 2.0 m, and the extension limit of the explosion fracture is 2.3 m. The gas phase change explosion is influenced by the coal roadway driving face, the gas content index and the analytical index of coal shavings. Experiments conducted for comparison also lead to the conclusion that the initial gas emission is increased by 3.7 times from the 100-meter borehole in the original coal mass after coalbed gas explosion anti-reflection.

KEYWORDS

Low-permeability; gas-rich; carbon dioxide; anti-reflection; gas explosion

1 Introduction

Coal plays an important role in the development of national economy [1,2]. With the depletion of coal resources in shallow reserves areas, the mining development of mines is gradually entering the deep zone where the coal seam is buried. The gas content of the coal seam is directly proportional to the thickness of the overlying bedrock, and the mines gradually transition to high-gas mines from the original low-gas mine due to gas emissions during the mine excavation process [3–5]. Because deep mines generally have several technical difficulties caused by poor permeability of coal seams, coal gas problems will present long-term constraints on the safety of coal production [6].

The problems of highly inefficient simultaneous extraction of coal and gas from low-permeability and high-gas coal seams in deep mines significantly restrict the sustainable development of coal industry [7,8]. To solve the permeability problem of the high-gas coal seams with low permeability under deep and complex geological conditions, the technology of liquid carbon dioxide (CO₂) phase change gas explosion for cracking and antireflection is proposed. The progress of research on CO₂ blasting, a method of rock



breaking that utilizes the rapid phase change of liquid carbon dioxide into gas to produce high-pressure shock waves, has been significant in recent years [9–11]. This method has the advantages of being environmentally friendly, safe, and cost-effective [12–14] compared to traditional blasting methods.

This study investigates the mechanism of anti-reflection in coal mass during CO₂ blasting and explores the effects of different parameters such as pressure, distance, and coal seam thickness on the blasting performance. The study uses a combination of theoretical analysis and experimental methods to provide a comprehensive understanding of the CO₂ blasting process. Compared with other research on CO₂ blasting, this study focuses specifically on the anti-reflection mechanism in coal mass, which is an important factor affecting the blasting performance. The study also explores the effects of different parameters on the blasting performance, providing valuable information for optimizing the CO₂ blasting process. Additionally, the study uses a combination of theoretical analysis and experimental methods, which enhances the reliability and accuracy of the results.

The basic principle of liquid CO₂ phase change blasting anti-reflection technology is to add liquid CO₂ of rated capacity into the cracker on the ground or in the downhole. After the filling is completed, a single cracker in series is placed in the blast hole, and the blasting of the crackers is started with the mining exploder from a long distance. The blast wave and blasting gas generated by the blasting directly act on the coal borehole wall to promote a large number of cracks in the coal mass and finally achieve the purpose of anti-reflection for the coal seam with low permeability [15–17].

As a new technology applied to coal mines, the inspection experiments on the anti-reflection mechanism and anti-reflection effect of liquid CO₂ phase change gas explosion anti-reflection technology for coal seams need to be further studied. The results of the study provide insight into the anti-reflection mechanism of coal under liquid CO₂ phase change gas explosion and demonstrate the potential of liquid CO₂ as an effective extinguishing agent in coal mines and other high-pressure environments. The findings also have broader implications for the development of safer and more effective fire suppression strategies in industrial settings.

2 Analysis of the Mechanism of Liquid Carbon Dioxide Phase Change Blasting

According to the theory of elasticity, it is known that the stress state at any point around a blast hole in a coal seam can be expressed as

$$\begin{cases} \sigma_{rrgeo} = -\frac{\sigma_{yygeo}}{2} \left[(1+k) \left[1 - \frac{r_b^2}{r^2} \right] - (1-k) \left(1 - \frac{4r_b^2}{r^2} + \frac{3r_b^4}{r^4} \right) \cos 2\theta \right] \\ \sigma_{\theta\theta geo} = -\frac{\sigma_{yygeo}}{2} \left[(1+k) \left[1 - \frac{r_b^2}{r^2} \right] + (1-k) \left(1 - \frac{4r_b^2}{r^2} + \frac{3r_b^4}{r^4} \right) \cos 2\theta \right] \\ \tau_{r\theta geo} = -\frac{\sigma_{yygeo}}{2} \left[(1-k) \left[1 + \frac{r_b^2}{r^2} - \frac{3r_b^4}{r^4} \right] \sin 2\theta \right] \end{cases} \quad (1)$$

In the formula, σ_{rrgeo} , $\sigma_{\theta\theta geo}$, $\sigma_{r\theta geo}$ are the state of stress at any point of the coal mass in polar coordinates; σ_{yygeo} is the vertical crustal stress component; K is the side pressure coefficient of horizontal crustal stress; θ is the angle between polar coordinates and horizontal direction.

There is a gap between the cracker and the blast hole, which is an uncoupled burst blast. The initial peak pressure of the blast hole can be expressed as follows:

$$p_c = \frac{1}{2(1+\gamma)} \rho_0 D_v^2 n \quad (2)$$

In the equation, ρ_0 is liquid carbon dioxide density at room temperature, kg/cm³; D_v is cracker blasting gas detonation speed, m/s; γ is the expansion adiabatic index of carbon dioxide phase-change detonation

products, usually $\gamma = 3$; n is the pressure increase coefficient of the detonation gas explosion, generally $n = 10$.

The mechanical model within the range of the fracture circle of the coal mass with borehole in the coal seam under gas explosion is shown in Fig. 1. In the figure, R_1 is the effective range of the fracture circle under gas explosion.

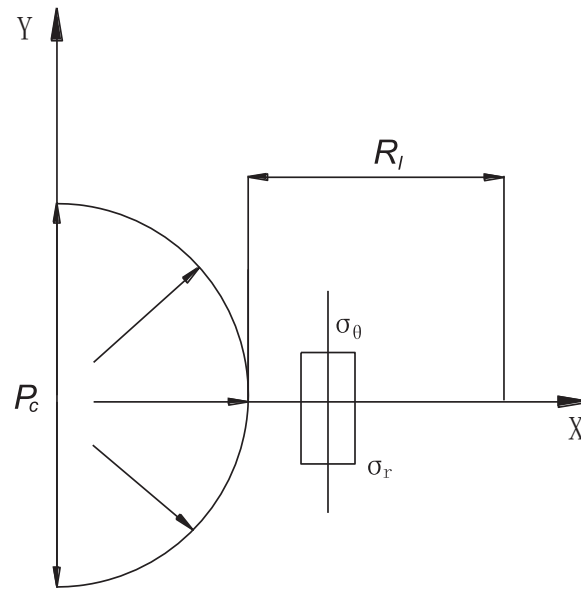


Figure 1: The mechanical model within the fracture circle range of the coal mass with borehole in the coal seam under gas explosion

The peak gas explosion pressure of liquid CO₂ phase change shows a big difference with explosives. It has been shown that liquid CO₂ phase change gas explosion is more difficult to form a large area of the crushing circle. This paper focuses on the study of the scope of the fracture circle formed by liquid CO₂ phase-change gas explosion. When the gas explosion shock wave decays into a compressive stress wave, the coal mass generates compressive stress and compressive deformation in the radial direction of coal mass. Tensile stress and deformation will also be produced from the tangential direction. Due to the poor tensile strength of the coal mass, when the tangential stress of the coal mass exceeds its tensile strength, a fracture will be generated in the radial direction.

There are studies showing that the gas shock wave attenuates very quickly in the coal mass and the peak pressure can be expressed as with the change rule of distance:

$$P(r) = P_c(\bar{r})^{-\alpha_s} \tag{3}$$

$$\bar{r} = r/r_b \tag{4}$$

$$\alpha_s = [2 - \mu / (1 - \mu)] \tag{5}$$

In the formula, \bar{r} is the specific distance; r is the distance from the explosion borehole; α_s is the attenuation coefficient of the shock wave in the crush zone; μ is Poisson's ratio of coal mass.

When the explosion shock wave propagates to the boundary of the compression zone, the shock wave decays into the form of a stress wave. According to the law of conservation of momentum, the pressure peak P_m at the edge of the impact zone of the coal mass is expressed as

$$P_m = \rho_c c_p v_r \quad (6)$$

In the formula, ρ_c is the density of coal mass, kg/m^3 ; c_p is a decay of the wave velocity of elastic stress wave, m/s ; v_r is the displacement velocity of coal rock mass at the edge of shock wave transmission, m/s ;

Based on the Poisson effect, the peak value of the tangential tensile stress generated by the gas explosion stress wave in the fracture region can be expressed as

$$\sigma_{\theta\theta\max} = P_m \left[\frac{\mu}{1-\mu} \left(\frac{r_b}{r} \right)^\alpha \right] \quad (7)$$

Since the peak stress value of the gas explosion in the fracture zone is greater than the peak value of the shock wave in the crush zone, considering the influence from the high ground stress suffered by the coal mass around the explosion borehole on the gas explosion crack, the total tangential stress on any point of the coal mass within the gas explosion fracture area can be expressed as

$$\sigma_{\theta\theta 1} = \sigma_{\theta\theta\max} + \sigma_{\theta\theta\text{geo}} = P_m \left[\frac{\mu}{1-\mu} \left(\frac{r_b}{r} \right)^\alpha \right] + \sigma_{\theta\theta\text{geo}} \quad (8)$$

Replace $\sigma_{\theta\theta 1}$ in formula (8) with the dynamic strength of extension of coal mass σ_{dt} , that is, to obtain the extension range causing the crack on radial direction after the gas explosion

$$r_c = r_b \left(\frac{\mu P_m}{(1-\mu)(\sigma_{dt} - \sigma_{\theta\theta\text{geo}})} \right)^{\frac{1}{\alpha}} \quad (9)$$

Therefore, the effective range of the coal mass fracture circle caused by liquid CO_2 phase change gas explosion is

$$R_l = r_c - r_b = r_b \left[\left(\frac{\mu P_m}{(1-\mu)(\sigma_{dt} - \sigma_{\theta\theta\text{geo}})} \right)^{\frac{1}{\alpha_s}} - 1 \right] \quad (10)$$

From the theoretical analysis and deduction, the effective range of the fracture circle formed around the blast hole under the action of phase change gas explosion is not only related to the peak pressure of the CO_2 cracker explosion, but also related to the stress resistance of the coal seam and the physical properties of the coal.

3 Study on the Numerical Simulation of the Carbon Dioxide Phase Change Cracking

The numerical simulation was targeted on the coal mass extracted from the No. 15203 working face in Area 2 of No. 15 Coal Seam, Mapu Mine, northeastern of Qinshui Coal Mine, Shanxi Province. The geometric model of the granular discrete element PFC^{2D} established is illustrated in Fig. 2. In the $16 \text{ m} \times 16 \text{ m}$ model, the boundary of the model was set as “wall” which played the role of the boundary of the model and particle escape protector after blasting at the central point. The peak pressure for the CO_2 phase-transition blasting was taken as 200 MPa in the numerical simulation.

In the simulation, the central point served as the blasting borehole, its diameter was set as 0.113 m, particle radius as 0.006–0.009 m, porosity of particle aggregate 0.1, and density of particle aggregate 1.521 kg/m^3 .

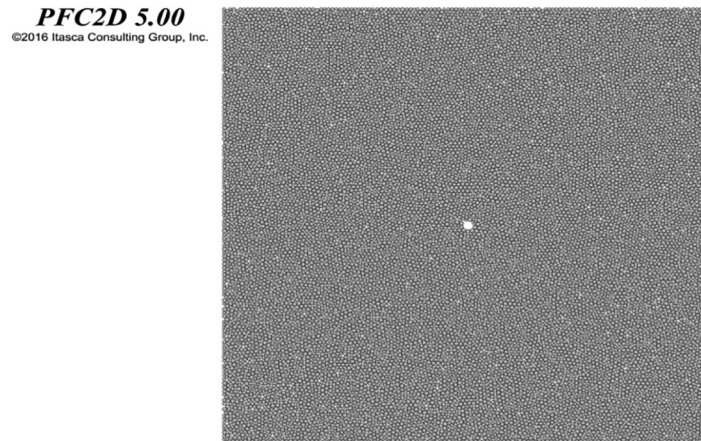


Figure 2: Geometric model of PFC^{2D}

The numerical simulation results shown in Fig. 3 reveal that the blasting gave rise to a 1 m wide crushed zone around the borehole, which means the destruction zone of the gas-rich coal seam resulting from the blasting is 1 m in radius; they also indicate that the maximum range of the secondary expanded zone of cracks from the blasting is 2 m, which means the damaged zone of the gas-rich coal seam is 1–2 m in radius, and the ultimate extension length of the explosion fracture is 2.3 m.

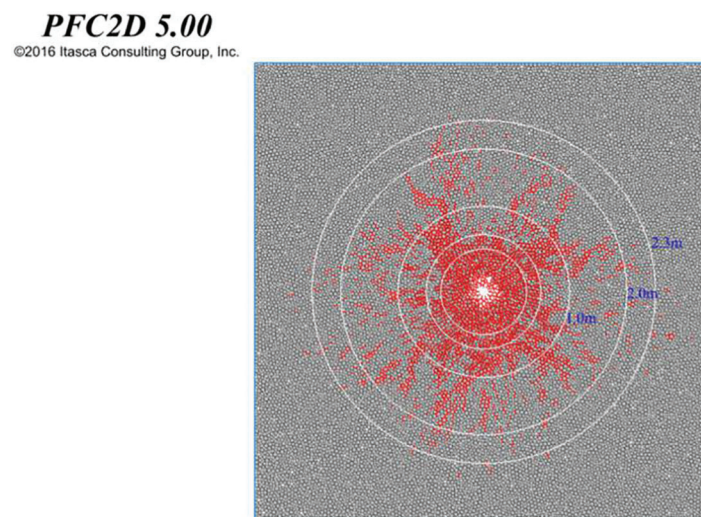


Figure 3: State of particles and fracture propagation after blasting

4 Field Test of Carbon Dioxide Phase Change Cracking

4.1 Experimental Work Surface Overview

An experimental study on the liquid CO₂ phase change gas-explosion-induced cracking anti-reflection in coal roadway heading face is implemented in the 15th coal seam 15203 wind crossheading coal roadway driving face. The distance of the working surface from the No. 9 coal seam is 47.24–71.63 m, and the average is 56.39 m. The thickness of the coal seam is 4.8–6.2 m, and the average thickness is 5.5 m, containing 0–3 layers of dirt band. The structure is relatively simple, and the recoverability index $K_m = 1$ with a variation coefficient of 18%. It is a stable and recoverable coal seam in the whole region, and the uniaxial compressive

strength is 17.5 MPa, while the uniaxial tensile strength is 0.86 MPa. The coal quality is ultra-low ash—medium-high ash, medium sulfur—high sulfur, low-to-moderate calorific value—extra-high lean coal (SM), meager lean coal (PS), and meagre coal (PM). The overall layout of the working face is a monoclinic structure, which leads to NNE, tends to NWW, and is expected to have a gradient of 0–4°, thus it is relatively flat. The driving face adopts a press-in type ventilation method, the method of gas drainage before excavation to control gas, and the pre-extraction time is 1 month. The original coal gas basic parameters measured before the gas-explosion-induced cracking anti-reflection experiment at the working face is implemented are presented in [Table 1](#).

Table 1: The original gas basic parameters of the experimental coal roadway driving face

Gas parameters	Gas content ($\text{m}^3 \cdot \text{t}^{-1}$)	Gas gushing amount per 100 m borehole ($\text{m}^3 \cdot (\text{min} \cdot \text{hm})^{-1}$)	Natural gas gushing attenuation coefficient/ d^{-1}	Gas pressure (MPa)	Seam permeability coefficient ($\text{m}^2 \cdot \text{MPa}^{-2} \cdot \text{d}^{-1}$)	Pre-extraction time (months)
Actual value measured	7.54	0.0865	0.035	0.57	1.32	1

4.2 Drilling Design for Carbon Dioxide Phase Change Cracking Test in Heading Face

In the No. 15203 coal roadway working face, the liquid CO_2 phase change gas-blast-induced cracking and anti-reflection experiment was carried out to improve the permeability of the coal mass ahead of the excavation and shorten the pre-extraction time of excavation face, thereby realizing coal road speedy drivage technology guided by liquid CO_2 phase change blasting. The maximum CO_2 burst pressure in the test can reach 200 MPa. A schematic diagram of the layout of the borehole of the gas blast experiment on the coal roadway driving face is shown in [Figs. 4 and 5](#). Test borehole construction parameter in [Table 2](#).

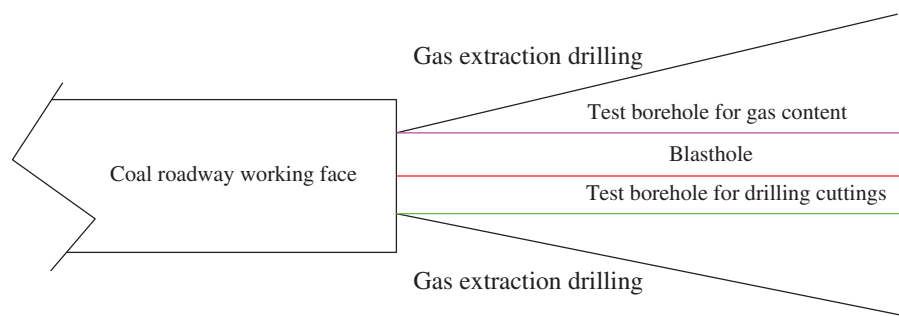


Figure 4: Borehole layout plane schematic of the gas-blast anti-reflection experiment on the coal mine roadway working face

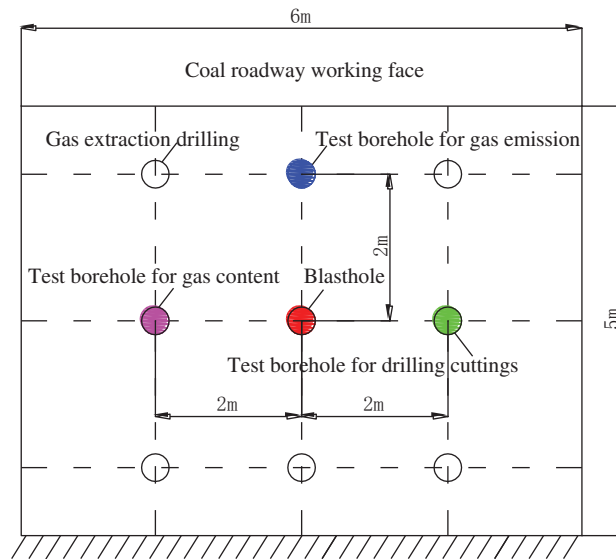


Figure 5: Borehole layout plane schematic of the gas-blast anti-reflection experiment on the coal mine roadway working face

Table 2: Test borehole construction parameter table

Borehole name	Hole height (m)	Bore diameter (mm)	Borehole depth (m)	Azimuth angle (°)
Blasthole	2.5	94	50	Vertical coal wall
Test borehole for gas content	2.5	94	50	Vertical coal wall
Test borehole for gas emission	4.5	94	50	Vertical coal wall
Test borehole for drilling cuttings	2.5	94	50	Vertical coal wall

4.3 Analysis of the Experimental Results of the Carbon Dioxide Phase Change Cracking in Heading Face

For this liquid CO₂ phase change gas-blast-induced cracking anti-reflection experiment in the coal seam driving face, the blasting depth is 50 m. Because the newly excavated working face does not have the problem of precluding the gas zone, the sealing depth is 7 m. After the gas blast anti-reflection test, extraction drill holes were connected for pre-drainage. After the gas explosion, the corresponding parameters of the test boreholes were tested daily to get the gas content W_h and the coal drilling cuttings analysis index Δh_2 . The SYQY-73 fixed-point rapid sampling equipment was used to measure the gas content, and the MD-2 coal-drill cutting gas analysis instrument was used to measure the analytical index of the coal cuttings, as shown in Fig. 6. A picture of the driving face before and after blasting in the coal mine heading is shown in Fig. 7. The blasting crushing radius is around 0.8 m based on the measurement.

Fig. 8 shows the gas content changing scheme with the pre-drainage time for whether the coal road heading driving face adopts the gas-explosion-induced cracking anti-reflection that the influence of the

negative pressure pre-drainage will gradually reduce the gas in the coal mass in the direction of coal roadway excavation. When the gas-explosion-induced cracking anti-reflection is not used, it will take 1 month for the pre-drainage to reduce the gas content of the raw coal to less than $5 \text{ m}^3/\text{t}$; when the gas-explosion-induced cracking anti-reflection is used, the reduction rate of gas content of the raw coal is significantly accelerated under the effect of pre-drainage. The gas content is reduced to less than $5 \text{ m}^3/\text{t}$ in about 15 days with pre-drainage. It can be determined that gas-explosion-induced cracking anti-reflection can increase the gas permeability of the coal and improve the pre-drainage efficiency of the coal seam, thereby achieving the goal of rapid excavation in a high-gas coal roadway with low permeability.



(a) MD-2 coal drilling cuttings desorber



(b) SYQY-73 fixed-point rapid sampling equipment

Figure 6: Field test device



(a) Before explosion



(b) After explosion

Figure 7: On-site picture of coal road heading driving face before and after blasting

The analysis index Δh_2 of coal drilling cuttings is an important index for judging the possibility of abnormal gas gushing ahead of the driving face. The detection index is widely used in high-gas and outburst mining face. The residual gas content (gas pressure) of the coal drilling cuttings collected at the fixed point is released into the confined space, and the volume of the confined space is used to represent the volume of gas resolved. As shown in Fig. 9, the gas-explosion-induced cracking anti-reflection has a greater influence on the analysis index of coal drilling cuttings, and after the gas explosion, its decreasing speed is faster after the gas explosion with pre-drainage time, and it decreases to a safety index of less than 200 Pa in about 16 days.

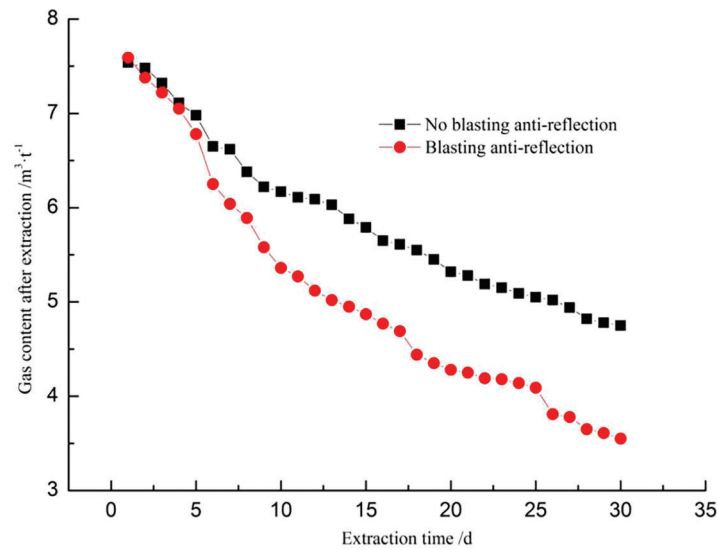


Figure 8: Variation in gas content before and after the blasting of coal road heading driving face

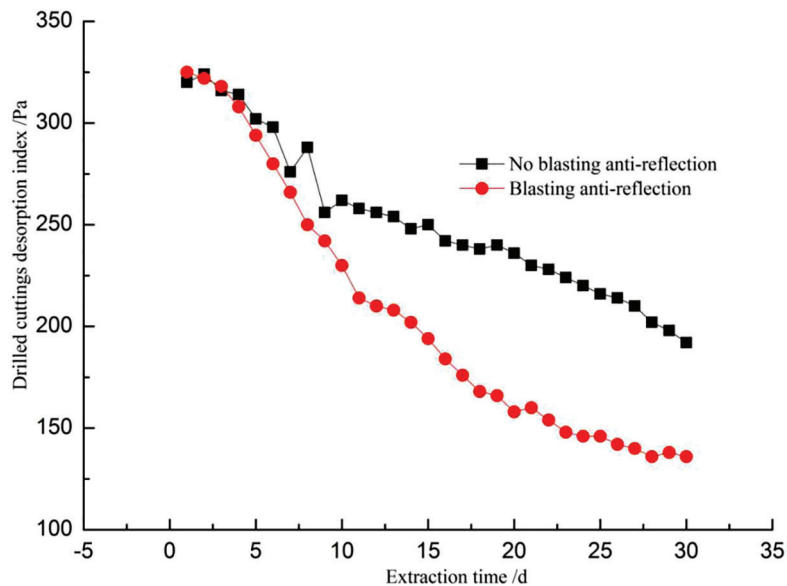


Figure 9: Variation of coal drilling cuttings analysis index before and after the blasting of coal road heading driving face with time

The attenuation curve of gas gushing from the coal seam borehole in the coal roadway diving face shown in Figs. 10 and 11 reveal that the initial gas gushing amount after coal seam borehole gas-explosion anti-reflection and 100 m test borehole drilled in the original coal mass are $0.3133 \text{ m}^3/\text{min}\cdot\text{hm}$ and $0.0865 \text{ m}^3/\text{min}\cdot\text{hm}$, respectively, and the natural gas gushing attenuation coefficients are 0.031 d^{-1} and 0.035 d^{-1} , respectively. From the measured results, it can be concluded that the initial gas gushing volume of the coal seam borehole gas-explosion-induced cracking anti-reflection is 3.7 times than the gas gushing volume of the original coal mass 100 m borehole without anti-reflection measure. The anti-reflection effect of gas-explosion phase change cracking is obvious. The attenuation coefficient of natural gas gushing is very small, which is determined by the desorption speed of the coal itself.

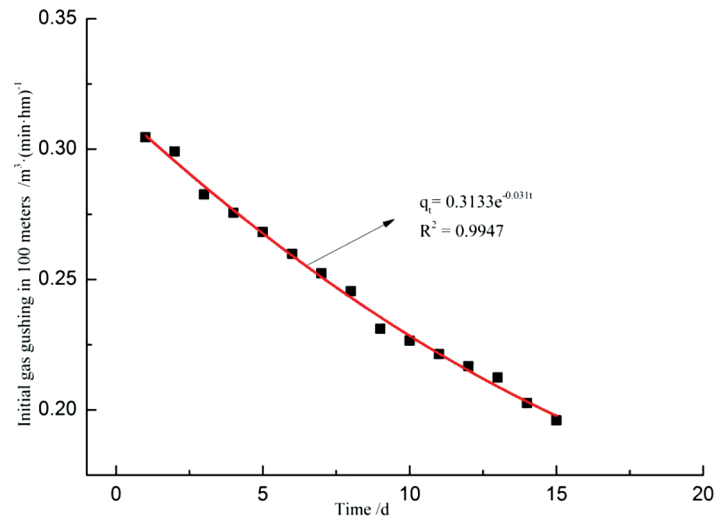


Figure 10: Attenuation curve of gas gushing from the gas-explosion controlling borehole in the coal roadway diving face

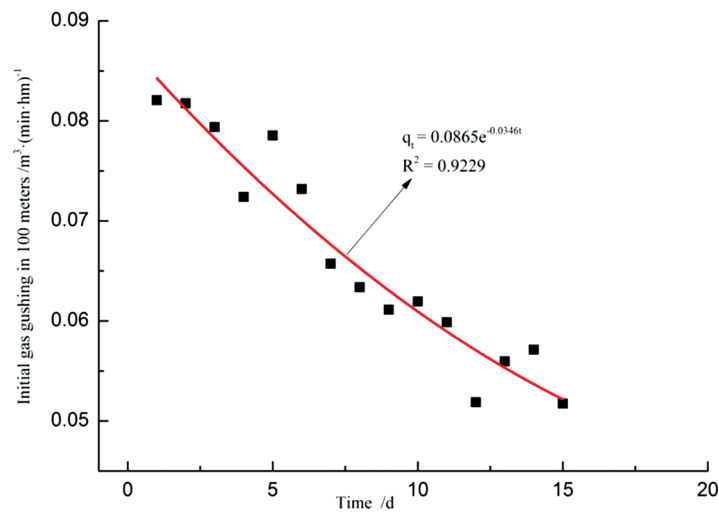


Figure 11: Attenuation curve of gas gushing from the original coal mass borehole in the coal roadway diving face

5 Conclusions

1. The formation mechanism of the coal mass fracture circle in liquid carbon dioxide gas phase change cracking is discussed in depth. The mathematical model of the fracture circle range is deduced theoretically. It is confirmed that the effective range of the fracture circle is related to the explosion venting peak pressure of the cracker, the coal seam stress, and the coal's physical parameters.
2. Numerical simulation analysis shows that the phase change gas explosion of liquid carbon dioxide causes a blasting crush zone with a radius of 1.0 m around the blast hole. The radius of the secondary expansion zone of the coal mass caused by the explosion gas is 2.0 m, and the ultimate extension length of the explosion fracture is 2.3 m.

3. After the liquid carbon dioxide phase change gas-explosion-induced cracking antireflection is adopted, the pre-drainage time required to reduce gas content to 5 m³/t is reduced from 30 days to 15 days, and the pre-drainage time required to reduce coal drill cuttings analysis index to 200 Pa is reduced from 30 days to 16 days.
4. The contrast test of coal seam borehole gas-explosion-induced cracking anti-reflection reaches a conclusion that the initial gas gushing volume of the 100 m coal seam borehole after gas-explosion anti-reflection is 3.7 times than that of the original coal, and the effect of the gas-explosion-induced cracking anti-reflection is obvious.

Funding Statement: This work was financially supported by the National Science and Technology Major Project (Grant No. 2016ZX05067004-003).

Conflicts of Interest: The authors declare that they have no conflicts of interest to report regarding the present study.

References

1. Wang, Q., Li, R. R. (2017). Decline in China's coal consumption: An evidence of peak coal or a temporary blip. *Energy Policy*, 108(9), 696–701.
2. Tang, E., Peng, C. (2017). A macro and microeconomic analysis of coal production in China. *Resources Policy*, 51(4), 234–242.
3. Yin, W. T., Fu, G., Yang, C., Jiang, Z. G., Zhu, K. et al. (2017). Fatal gas explosion accidents on Chinese coal mines and the characteristics of unsafe behaviors. *Safety Science*, 92(2), 173–179.
4. Jin, K., Cheng, Y. P., Wang, W., Liu, H. B., Liu, Z. D. et al. (2016). Evaluation of the remote lower protective seam mining for coal mine gas control: A typical case study from the Zhuxianzhuang Coal Mine, Huaibei Coalfield, China. *Journal of Natural Gas Science and Engineering*, 33(7), 44–55.
5. Durant, B., Abualfaraj, N., Olson, M. S., Gurian, P. L. (2016). Assessing dermal exposure risk to workers from flowback water during shale gas hydraulic fracturing activity. *Journal of Natural Gas Science and Engineering*, 34(8), 969–978.
6. Huang, B. X., Cheng, Q. Y., Chen, S. L. (2016). Phenomenon of methane driven caused by hydraulic fracturing in methane-bearing coal seams. *International Journal of Mining Science and Technology*, 26(5), 919–927.
7. Lei, Y., Liu, J. J., Zhang, S. N., Zhang, W., Wang, H. D. (2017). Contrast test of different permeability improvement technologies for gas-rich low-permeability coal seams. *Journal of Natural Gas Science and Engineering*, 33(7), 1282–1290.
8. Zou, Y. M. (2019). Study on the coal seam permeability increasing technique based on hydraulic cutting and CO₂ fracturing. *Coal Science and Technology*, 47(1), 226–230.
9. Zhang, X. G., Jiang, W. Z., Du, F. (2021). Development status and prospect of permeability enhancement technology in high gas low permeability coal seam. *Safety in Coal Mines*, 52(2), 169–176.
10. Chen, H. D., Wang, Z. F., Chen, X. E., Chen, X. J., Wang, L. G. (2017). Increasing permeability of coal seams using the phase energy of liquid carbon dioxide. *Journal of CO₂ Utilization*, 19(5), 112–119.
11. Cao, Y. X., Zhang, J. S., Zhai, H., Fu, G. T., Tian, L. et al. (2017). CO₂ gas fracturing: A novel reservoir stimulation technology in low permeability gassy coal seams. *Fuel*, 203(9), 197–207.
12. Lei, Y., Liu, J. J., Zhang, S. N. (2017). Research on permeability improvement technology of CO₂ phase transition crack the coal seam. *Journal of Engineering Geology*, 25(1), 215–221.
13. Cohen, F., Valacchi, G. (2022). The heterogeneous impact of coal prices on the location of cleaner and dirtier steel plants. *The Energy Journal*, 43(2), 187–189.
14. Kerstin, M. (2021). Breaking the dichotomies: Climate, coal, and gender. Paving the way to a just transition. The example of Colombia. *Energies*, 14(17), 5457.

15. Jochen, M., Adrian, R., Linda, W. (2021). Analyzing transitions through the lens of discourse networks: Coal phase-out in Germany. *Environmental Innovation and Societal Transitions*, 40(9), 315–331.
16. Abdul, R., Ma, H. Y., Magdalena, R., Ileana, S. C., Zahid, Y. (2021). Energy crisis in Pakistan and economic progress: Decoupling the impact of coal energy consumption in power and brick kilns. *Mathematics*, 9(17), 2083.
17. Sergey, Z., Michal, C. (2021). Coal mining sustainable development: Economics and technological outlook. *Energies*, 14(16), 5029.